UNIVERSITY OF MINNESOTA
Driven to Discover℠

Suite 1000 ME
111 Church St. SE
Minneapolis, MN 55455-0111

Project Title: Embedded Nanocrystal Silicon Films: A New Paradigm for Improving the Stability of Thin-film Silicon

Contract Number: RD-3-25 **Milestone Number:** 7 **Report Date:** 30 Aug 2010

Principal Investigator: Uwe Kortshagen 612-625-4028

Contract Contact: Any Rollinger 612-625-1359

Congressional District: (Corporate office) Minnesota 5th

Congressional District: (Project location) Minnesota 5th

MILESTONE REPORT

Executive Summary:

More than 90% of the market share of all photovolatics (PV) modules sold in 2005 were based on crystalline or amorphous silicon. The problem faced by silicon (Si) PV technology, as well as any other PV-technology, is that the electricity generated is about a factor of five too expensive to be competitive with that obtained from conventional coal-fired power plants. Under this grant, we pursue two different routes that may help increase the efficiency and lower the cost of silicon solar cells. Our first approach **(Track 1)** is based on our unique ability to produce silicon nano-crystals in a low-pressure plasma-based synthesis reactor and to embed these nano-crystals in amorphous silicon films. Our novel deposition process enables us to independently control the properties of the amorphous matrix and of the crystalline phase, which we hope will enable us to improve the electronic quality of amorphous silicon that is used in thin film solar cells. In the second approach **(Track 2)**, we study using such embedded nano-crystals as nuclei for seed-induced re-crystallization of amorphous silicon films. We expect that controlling the seed concentration will enable us to grow microcrystalline Si films faster and with grain sizes larger than possible with other deposition approaches. This may enable the cheaper production of solar cells based on microcrystalline silicon.

During this quarter, studies in track 1 focused on characterizing the electronic properties of amorphous silicon thin films with embedded nanocrystals. The electronic structure of these mixed-phase films was explored with conductivity and thermopower measurements. Briefly, one typically measures different activation energies for thermopower and conductivity in amorphous semiconductors and this difference is generally ascribed to the potential fluctuations that are believed to exist in the material. As the conductivity is determined from a closed circuit measurement, the electrons must surmount the largest potential fluctuation they encounter, while for thermopower measurements in open circuit, this is not the case.

In track 2 efforts were focused primarily on micro-scale understanding of the crystallization process through an investigation of secondary trends suggesting “seed competition based” growth behavior as well as a more in-depth and quantitative characterization of the film stress state induced by seeding. Our studies suggest that while higher initial seed concentrations lead to faster initial crystal growth, the crystal growth speed for these films is smaller than for those with lower seed density. Measurements of the film stress showed that compared to the stress

values observed in literature for unseeded silicon films, the intrinsic tensile stress of the seeded films exhibited a much higher magnitude due to the existence of extrinsic seeds.

Project funding provided by customers of Xcel Energy through a grant from the Renewable Development Fund.

Technical Progress:

Both tracks of the project have made good progress and achieved the milestone set in the contract. The progress made on both tracks will be discussed below.

Track 1: ***Embedded nanocrystals in amorphous silicon***

Within this research track, we are continuing to study the effects of the embedded silicon nanocrystals in hydrogenated amorphous silicon. This quarter, we have shifted focus from the optical properties to the electronic properties of the mixed phase amorphous/nanocrystalline films (a/nc-Si:H). Previous measurements of the conductivity already revealed interesting results [1] and this quarter we present the first measurements of thermopower (also known as the Seebeck coefficient) in a/nc-Si:H. As described in the first quarterly report (Q1), a dual plasma system has been used to produce silicon nanocrystals in one plasma deposition system. The particles generated in this system are then entrained by a carrier gas and injected into a second plasma deposition system. These nanocrystals are embedded into a hydrogenated amorphous silicon film being grown in a second plasma.

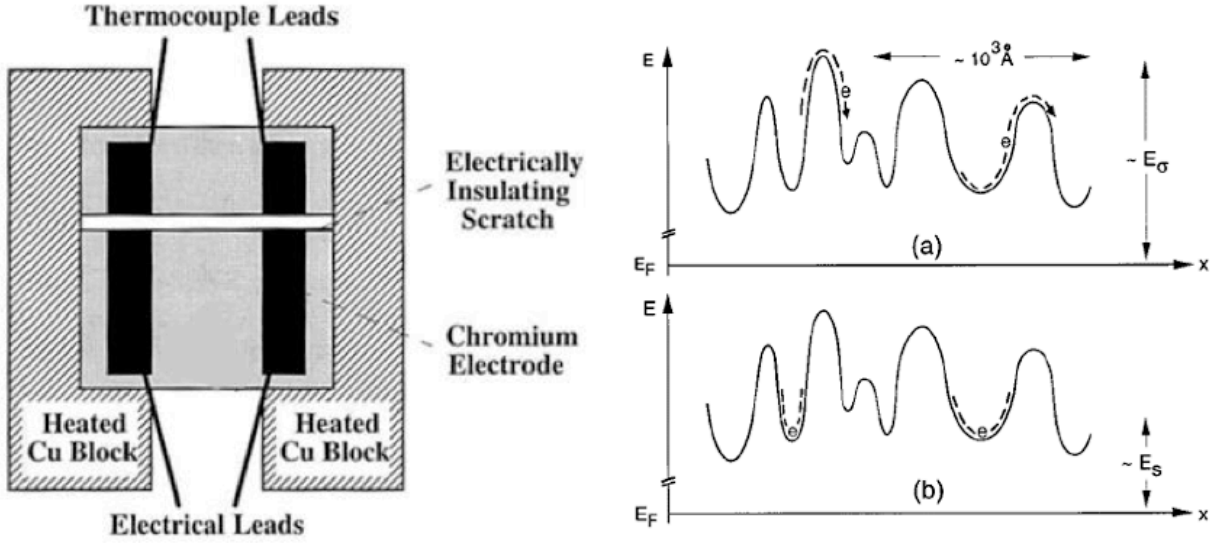

Figure 1a: The thermopower measurement system. 1b: The potential energy landscape of a-Si:H.

Thermopower measurements are based on the Seebeck effect; when a temperature gradient is applied to a metal or semiconductor, charge carriers are transferred between the hot and cold ends. When the measurement is done in open circuit mode, a voltage difference is developed; in closed circuit, a current flows. Generally, the voltage difference is measured as a function of temperature and will display an activated behavior for amorphous semiconductors. A sketch of the measurement system can be seen in figure 1a. There are two copper blocks, sepa-

rated by a gap, with the film bridging the gap between the blocks. The temperature of each block can be independently controlled by a heater/thermocouple combination to create a hot side of the film at temperature T_{hot} and a cold side at T_{cold}. Several temperature differences can be measured at each average temperature, $(T_{hot}+T_{cold})/2$, to ensure that the voltage is linear with the applied temperature difference.

The thermopower in amorphous semiconductors has provided a great deal of insight into the transport mechanisms [2], because it provides an alternate and complimentary method of probing the charge transport. Briefly, one typically measures different activation energies for thermopower and conductivity in amorphous semiconductors and this difference is generally ascribed to the potential fluctuations that are believed to exist in the material. As the conductivity is determined from a closed circuit measurement, the electrons must surmount the largest potential fluctuation they encounter, while for thermopower measurements in open circuit, this is not the case. A cartoon of this situation can be seen in figure 1b, with E_S and E_σ being the activation energies for thermopower and conductivity respectively.

In figure 2, we present the thermopower and conductivity measurements for a few of the a/nc-Si:H films, as well as an undoped a-Si:H and doped a-Si:H film for comparison. Due to the large difficulty in measuring such small voltages (~1 mV) across high impedance films (50 – 200 GΩ at 350K) only a few films could be measured. In table 1, the activation energies for both conductivity and thermopower as well as the activation energy, ΔE, are listed. The mixed phase films are denoted by their respective crystal fraction (XC).

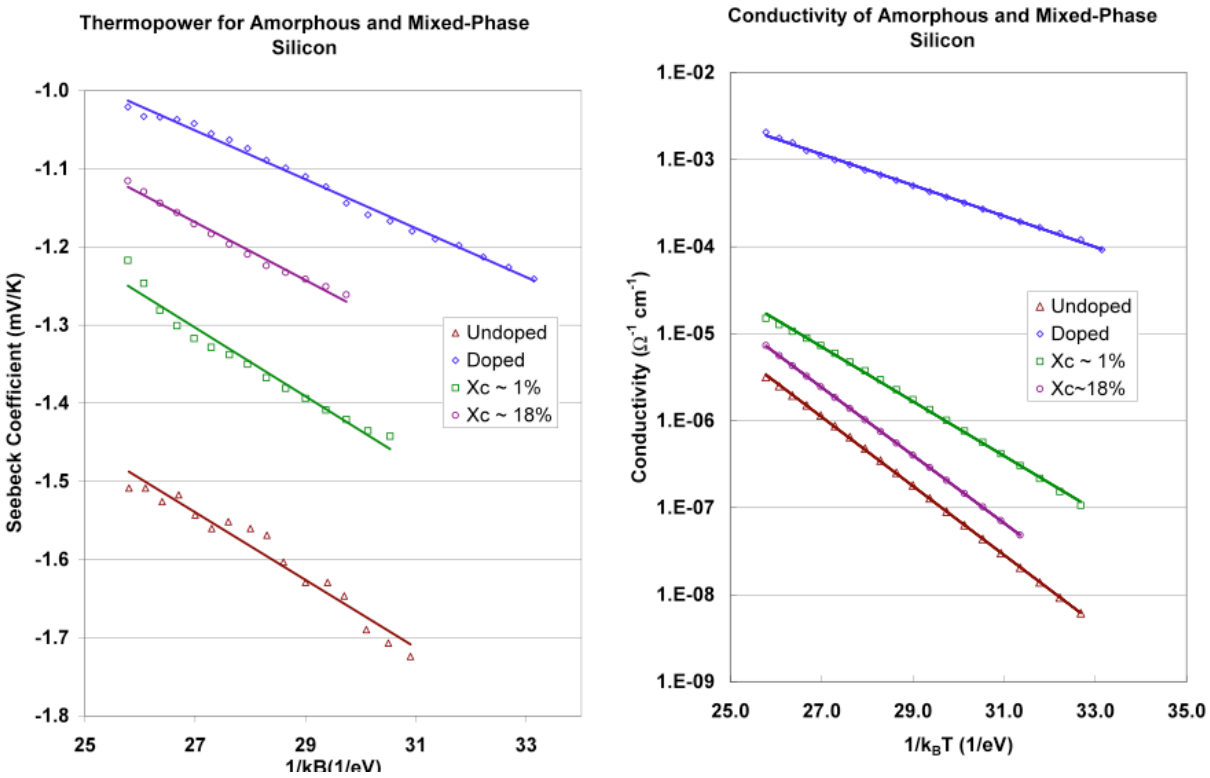

Figure 2: Plots of the thermopower (left) and conductivity (right) for two films of differing crystal fractions with a doped and undoped a-Si:H sample for comparison.

Film	Undoped	6*10-5 [PH3/SiH4]	XC ~ 1%	XC ~ 18%
E_σ (eV)	0.91	0.41	0.90	0.72
E_S (eV)	0.50	0.36	0.43	0.45
ΔE (eV)	0.41	0.05	0.47	0.27

Table 1: The different activation energies for each film.

Efforts are underway to measure doped mixed-phase films, to be presented in the next quarterly report. As the impedance of the doped films is lower, we should be able to ascertain the Seebeck coefficient for a broader range of mixed phase films.

Track 2: ***Large-grain re-crystallized Si***

The second track of the project aims at controlling the grain structure and reducing the re-crystallization time of micro-crystalline films through the annealing of amorphous silicon films in which silicon nano-crystals are embedded as "seeds" for crystal grain growth. In quarter 6, efforts on the macroscopic front of seeded film application and performance focused mainly on enhancing the conductivity of seeded, recrystallized films through successful development of a customized hydrogen grain boundary treatment procedure. On the microscopic front, the continuing effort to understand the unique science of this new crystallization process continued with studies revealing more about important stress effects induced by the embedded seeds on their surrounding film. In quarter 7, efforts were focused primarily on micro-scale science of the crystallization process through an investigation of secondary trends suggesting "seed competition based" growth behavior as well as a more in-depth and quantitative characterization of the film stress state induced by seeding.

As discussed in the summaries of quarters 5 and 6, a very interesting and unexpected secondary trend emerged in the crystallization kinetic plots of seeded films suggesting that a "competition-based" behavior dictates the growth of embedded seeds. Films containing relatively dense populations of seed crystals, and thus more growth sites for crystallization to originate from, are intuitively expected to achieve full re-crystallization before those with fewer initial seeds. However, the first study of crystal growth rate vs. seed density in quarter 5 consisting of a comparison of films containing three different initial seed densities, gave evidence to suggest otherwise. Specifically, although the most heavily seeded film followed the expected behavior of being first to achieve full recrystallization, the most sparsely seeded film showed faster recrystallization than the film having a seed density of "medium" concentration.

This behavior suggests that, within a certain range of initial seed densities, more heavily seeded films might create an environment in which crystal growth is hindered due to closely spaced seeds having to compete for growth space. In order to investigate this hypothesis further, another study of crystallization rate vs. initial seed population density was performed, this time comparing three seeded films spanning a wider range of initial seed densities, so as to reduce potential scatter. All three samples were annealed in simultaneous intervals along with a fourth un-

seeded control sample, with their initial seed population densities confirmed by atomic force microscopy (AFM) measurements. Both AFM and crystallization rate results are depicted in figure 3 below, where a very clear trend emerges corroborating the competition based growth behavior that was subtly suggested by quarter 5's analogous study. Indeed, although samples having lower seed population densities initially lag behind more heavily seeded samples, beyond a certain point in the annealing process they appear to "accelerate" past more heavily seeded samples in crystal volume fraction.

It is also interesting to note that the inflection point at which this appears to occur is between crystal fractions of 10-15%. This is very near the range of crystal fractions commonly referred to in solid-phase crystallization literature as the "percolation threshold", or the minimum crystal volume fraction which must be present in order for nucleation sites to be able to connect to form large grain networks [3,4]. This further supports the hypothesis that seed growth is dictated by competition, as it would make sense that the inflection point would occur near crystal fractions in which adjacent growth sites would be able to achieve significant contact.

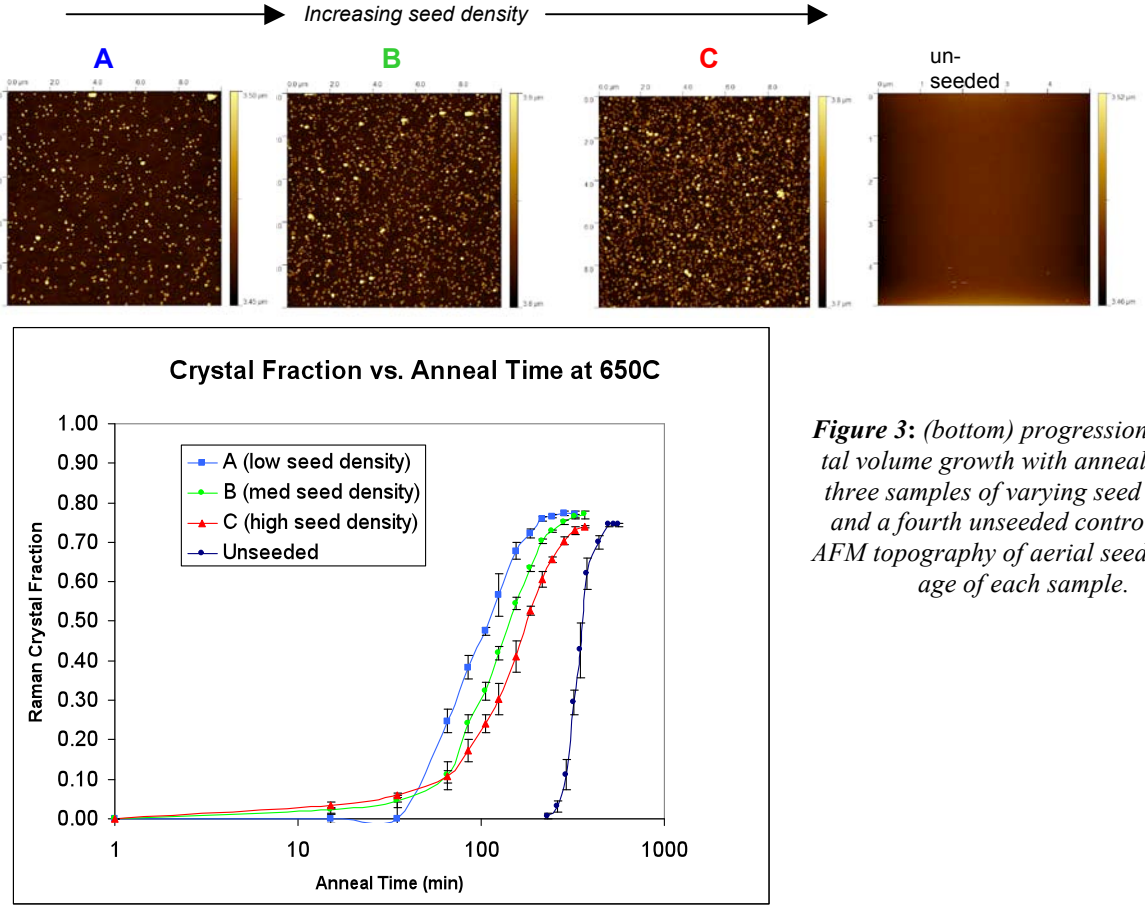

***Figure 3**: (bottom) progression of crystal volume growth with anneal time of three samples of varying seed density and a fourth unseeded control, (top) AFM topography of aerial seed coverage of each sample.*

Of the several factors of film composition that affect crystal growth in an amorphous silicon film, film stress is perhaps the most important structural influence. With seeded films specifically, the stress induced by the embedded crystals on the surrounding amorphous film may be another key factor in the competition-based growth behavior observed in the crystallization kinetics. In quarter 6 studies of film stress focused on visual, scanning electron microscopy (SEM) analysis of the geometric effects of seed embedding on the amorphous film, showing that embedded seeds appeared to produce conic regions of stress in the surrounding film environment. In

quarter 7, in-depth quantitative studies of the film stress state were carried out for seeded films of varying hydrogen content, for various stages in the annealing process. Comparison of samples having various initial hydrogen concentrations was of interest because it is believed that the crystallization of a-Si:H films is strongly dependent on the hydrogen content, which is related to the residual stress in the film [5-7]. The thermal energy provided by annealing is used to relieve the initial stress in the film and initiate the crystallization process. The total stress is calculated by the Stoney equation [8]:

$$\sigma_T = \frac{E_S t_S^{\,2}}{6(1-\nu_S)Rt_F},$$

where E_S is the Young's modulus of the substrate, t_S is the substrate thickness, υ_S is Poisson's ratio of the substrate, R is the beam radius of curvature and t_F is the film thickness. Several mechanisms can contribute to the total film stress. The primary component is the intrinsic stress σ_i, which is produced by film growth processes and defects in film structure. Two remaining contributors are external stress and thermal stress. External stress, which can be introduced during film processing and handling, is kept negligible. The thermal stress, which arises from the difference between the thermal coefficients of expansion of the substrate and the film, can be subtracted from the measured total stress to yield the intrinsic stress σ_i [9],

$$\sigma_i = \sigma_T - \frac{E_F(\alpha_S-\alpha_F)(T_d-T_m)}{(1-\nu_F)},$$

where E_F is the Young's modulus of the film, υ_F is the Poisson's ratio of the film, α_S and α_F are the thermal coefficients of expansion for the substrate and film, respectively, and T_d and T_m are the deposition and curvature measurement temperatures. The values of the physical parameters in equations above are as follows: $E_S = 7.09\times10^{10}$Pa, $\upsilon_S = 0.23$, $\alpha_S = 3.76\times10^{-6}{}^{\circ}C^{-1}$, $E_F = 17\times10^{10}$Pa, $\upsilon_F = 0.22$, and $\alpha_F = 0.40\times10^{-6}{}^{\circ}C^{-1}$.

The film curvature is measured by profilometer and calibrated with the bare substrate curvature. The residual stress variation of amorphous silicon during annealing (600 °C) has been reported in literature [10], where a transition from highly compressive to highly tensile stress is shown including an initial rapid increase, a period of latency, a quasi-linear increase and a final level. The initial rapid increase has been explained due to dehydrogenation effects at the begin stage of annealing. The next two steps correspond to the incubation period and the volume contraction during crystallization phases, respectively. Finally when the silicon film is completely crystallized, the stress stays constant (roughly 400Mpa).

The local residual stress in μc-Si:H film could also be calculated using Raman spectrometry in resonance with the silicon direct band gap [11], where a spatial resolution of less than 1μm can be obtained. Compared to profilometer probes, Raman measurement has certain advantages or features.

First, Raman frequency shifts, caused by residual stress in silicon film are usually very small, with a Raman shift of about $0.08cm^{-1}$ typically corresponding to 40MPa stress variations [12], which indicates better accuracy. Also Raman has better spatial resolution on the micrometer scale, which could avoid the effect of the substrate and thermal stress.

Mechanical strain may affect the frequencies of the Raman modes, or:

$$\sigma(\mathrm{Mpa}) = -250\Delta\omega(\mathrm{cm}^{-1}),$$

where $\Delta\omega = \omega_s - \omega_0$. ω_0 is the wave number of the stress free single crystal (520.5cm^{-1}) and ω_s is the wave number of the stressed sample. A peak shift towards lower wave numbers indicates tensile stress, and a shift towards higher wave numbers is related to compressive stress.

The laser beam in Raman measurement can cause local bulk heating of the investigated area, which causes a peak shift to lower wave numbers; similar to tensile stress. Thus the laser power should not exceed 2.5mW to keep the tensile stress due to local heating below 0.01cm^{-1}. Also the integration time should be long enough to provide sufficient signal to noise (S/N) ratio for accurately fitting the Raman peak with a Lorentz curve.

The total stress in seeded silicon films before and after annealing is measured using a Tencor P10 profilometer, where the film curvature is calculated from the surface roughness. A preliminary study on the variation of residual film stress throughout the annealing process was carried out on three films of equivalent seed density and composition, but of varying initial hydrogen content (achieved through variation of film deposition temperature). The intrinsic stress of seeded films was calculated by subtracting the thermal stress from total stress. Compared to the stress values observed in literature for unseeded silicon films, the intrinsic tensile stress of the seeded films exhibited a much higher magnitude due to the existence of extrinsic seeds. Seeded films do exhibit a behavior similar to literature reported unseeded films, however, in terms of a decreasing stress with anneal time. Figure 4 below shows the results of this study, with the red plots showing the progression of film stress throughout the annealing process, and the blue plots show the corresponding Raman crystalline fraction.

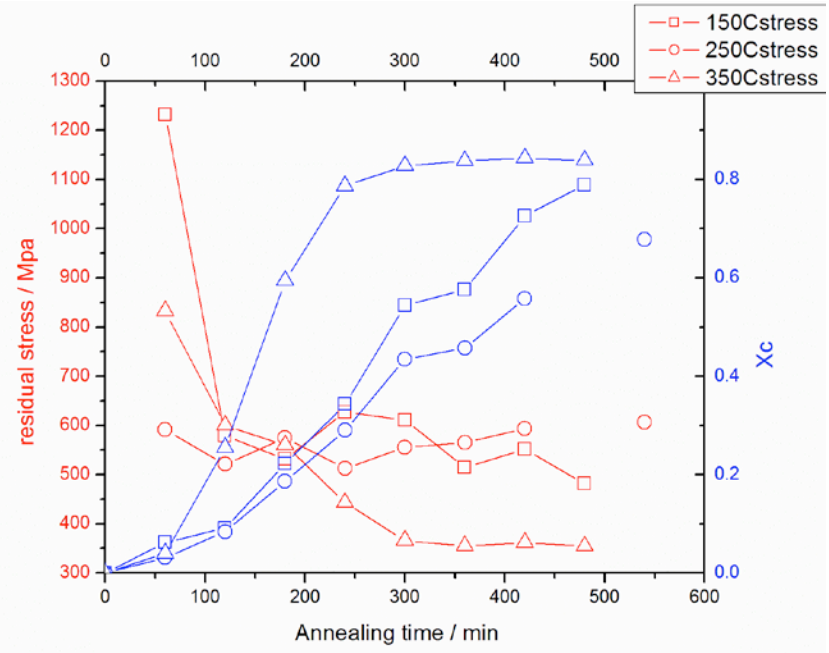

***Figure 4**: Time-series plots of Raman crystalline fraction & residual stress vs. annealing time for seeded films at different deposition temperatures*

In conclusion, the studies completed in quarter 7 have produced significant insights into the parameters affecting the unique growth kinetics of seeded films. Since maximization of grain size (and essentially electronic transport) while minimization of annealing time is ultimately a desired result of this effort, this quarters results showing lower seed density films exhibiting faster recrystallization is evidence that these two goals may not be as mutually exclusive as ex-

pected. Furthermore, new insight into the interlinked roles of hydrogen and film stress of seeded films has been quantitatively characterized, with studies currently underway to characterize the effects of varying seed population density on film stress. As stated in quarter 6, studies focused on characterizing the variation of electrical transport properties across the film are near completion, along with studies attempting to characterize the extent and nature of grain boundary and grain structure influences on the electronic properties within recrystallized films.

Project Presentations: Two separate presentations showcasing results from the recent track 2 studies were presented at the 2010 Gordon Conference on Plasma Physics within the last quarter.

Additional Milestones: Work is in progress towards milestone 8.

Project Status: The project is on schedule.

Milestone 7

To be completed 21 months after the Contract Start Date

Track 1: Embedded nanocrystal amorphous Si – Continue to establish main parameters affecting optical and electronic properties of the embedded nanocrystal amorphous films. Begin determining effect of amorphous matrix deposition conditions on film properties for given nanocrystal size and density.

Track 2: Large-grain recrystallized Si - Continue to establish main parameters affecting the crystal growth kinetics, incubation time, and grain size distribution. Begin to determine influence of hydrogen-content of amorphous matrix on recrystallization.

Deliverable 7

Submission of conference paper or technical lecture. Submission of Milestone Report detailing completion of Milestone 7 requirements to RDF representative.

References:

1. Y. Adjallah, C. Anderson, U. Kortshagen, and J. Kakalios, *Structural and electronic properties of dual plasma codeposited mixed-phase amorphous/nanocrystalline thin films*, J. Appl. Physics **107**, 043704 (2010).
2. H. M. Dyalsingh and J. Kakalios, *Thermopower and conductivity activation energies in hydrogenated amorphous silicon,* Phys. Rev. B **54**, 7630 (1996).
3. M. Ledinsky, A. Vetushka, J. Stuchlik, T. Mates, A. Fejfar, J. Kochka, J. Stepanek, *Crystallinity of the mixed phase silicon thin films by Raman spectroscopy* J. of Non. Cryst. Solids, **354** (2008): 2253-2257.
4. H. Overhof, M. Otte, M. Schmidtke, U. Backhausen, R. Carius, *The transport mechanism in micro- crystalline silicon. J. of Non. Cryst. Solids, 1998. **227-230**: p. 992-995.*
5. W Beyer, H Wagner 1983, "The Role of hydrogen in aSi:H- Results of evolution and annealing studies"*, J. Non-Cryst. Solids*. **59-60**, 161-168.
6. G Haberke, L Krausbauer, E F Steigmeier, A E Widmer, H F Kappert, G Neugebauer 1982, "High quality polysilicon by amorphous low pressure chemical vapor deposition"*, Appl. Phys. Lett.* **42** (3), 249-251.
7. P Danesh, B Pantchev, K Antonova, E Liarokapis, B Schmidt, D Grambole and J Baran 2004, "Hydrogen bonding and structural order in hydrogenated amorphous silicon prepared with hydrogen-diluted silane"*, J. Phys. D: Appl. Phys*. **37**, 249-254.
8. Maruf Hossain, H.H.A.-S., Hameed Naseem, and William D. Brown, "Effect of stress on the aluminum-induced crystallization of hydrogenated amorphous silicon films", *J. Mater. Res.*, 2006. **21**(10): p. 2582-2586.

9. P. H. Townsend, D.M.B., and T. A. Brunner, “Elastic relationships in layered composite media with approximation for the case of thin films on a thick substrate”, *Journal of Applied Physics,* 1987. **62**(11): p. 4438-4444.
10. P. Temple-Boyer, E.S., G. Faugere, B. Rousset, ”Residual stress in silicon films deposited by LPCVD from disilane”, *Thin Solid Films*, 1997. **310**: p. 234-237.
11. Thanh Nga Nguyen, V.D.N., Sungwook Jung, Junsin Yi, “Raman scattering analysis of the residual stress in metal-induced crystallized amorphous silicon thin films using nickel”, *Applied Surface Science*, 2009. **255**(19): p. 8252-8256.
12. Wolf, I.D., “Micro-Raman spectroscopy to study local mechanical stress in silicon integrated circuits”, *Semiconductor Science and Technology*, 1996. **11**(2): p. 135-154.

Appendix A

Conference poster presentations presented at the 2010 Gordon Research Conference on Plasma Processing Science, Colby-Sawyer College, New London, NH, July 11-16, 2010.

Crystallization Enhancement of Amorphous Silicon Films with Embedded Silicon Nanoparticles

Lin Cui, Jason Trask, Andrew Wagner, Curtis Andersen, Uwe Kortshagen

Motivation

· Improvements in the efficiency and the stability of amorphous Si thin-film cells have been achieved by controlling the micro-structure of the amorphous hydrogenated silicon.

· A new technique is developed by embedding nanocrystals in amorphous silicon films as nuclei for seed-induced crystallization.

· The layer-by-layer method enables elimination of amorphous incubation time and fast production of polycrystalline Si films with maximum possible grain size.

Schematic of "dual plasma" system

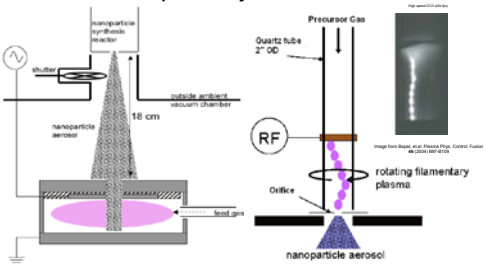

Left: Schematic of dual plasma chamber.

Right: Schematic of nanoparticle synthesis plasma chamber used to produce 20-30 nm single crystals.

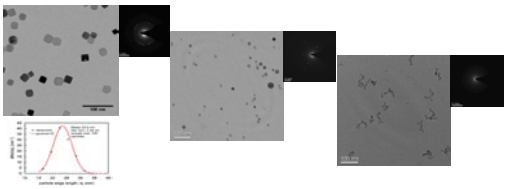

Left: Cubic Nanocrystals. (4 sccm Ar, 3 sccm SiH4/He, 140W RF, 1mm orifice, Filamentary mode) (From Curtis Anderson. PhD thesis, 2008)
Middle: Spherical Nanocrystals. (2 sccm Ar, 6 sccm SiH4/He, 130W RF, 1mm orifice, Diffusion mode)
Right: Amorphous particles. (4 sccm Ar, 3 sccm SiH4/He, 10W RF, 2 mm orifice, Diffusion mode)

Seeded Film Measurement

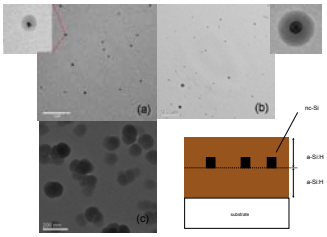

TEM images of as-deposit films:

(a) Bright-field TEM image of cubic nc-Si embedded into a-Si:H film.

(b) Bright-field TEM image of spherical nc-Si embedded into a-Si:H film.

(c) Bright-field TEM image of a-Si particles embedded into a-Si:H film.

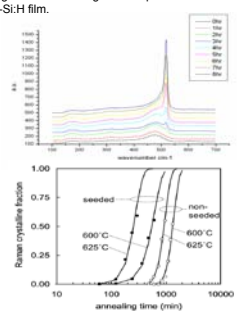

Top: Time series of confocal Raman spectra of a-Si:H film embedded with cubic nc-Si. (T=650℃, furnace annealing)

Bottom: Kinetic plots of Raman crystalline fraction vs. annealing time for seeded and non-seeded films at two annealing temperatures.

Enhanced crystallization mechanism

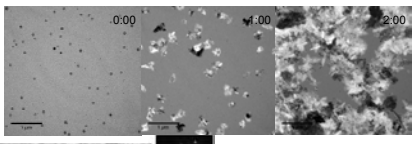

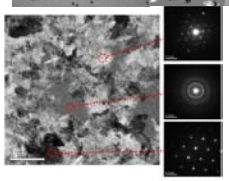

Top: Time series of heating stage TEM images of a-Si:H film embedded with cubic nc-Si annealed at 650℃.

Left: Bright-field TEM image after 2.5 hours annealing at 625˚C, showing selected area electron diffraction. TEM reveals growth of seed particles dominates recrystallization and native nucleation in bulk a-Si not largely observed. (From Curtis Anderson. PhD thesis, 2008)

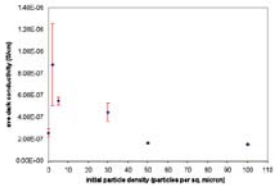

Dark conductivity vs. initial seed density for annealed films having various initial seed densities, along with an unseeded control film.

Key Results

1 Manage to seed amorphous Si film with different types of silicon nanocrystals which eliminate the amorphous incubation time during crystallization.

2 Independently control the properties of the amorphous matrix and the crystalline phase, including crystal fraction of the film as well as the size of the embedded nanocrystals.

3 Maximization of crystal growth speed and grain size, and other film properties including further electrical characterization in progress.

Acknowledgements

This work was partially supported by NSF grants DMR-0705675, NER-DMI-0403887, IGERT grant DGE-0114372, and Xcel Energy Renewable Development Fund grant RD-3-25, and parts of this work were carried out in the Institute of Technology Characterization Facility, University of Minnesota, a member of the NSF funded Materials Research Facilities Network (www.mrfn.org).

High Temperature and Plasma Lab
Mechanical Engineering

University of Minnesota
Driven to Discover℠

Seed Enhanced Crystallization of Amorphous Silicon

Jason Trask[1] ; Andrew J. Wagner[2] ; Lin Cui[1] ; Uwe Kortshagen[1]
[1] Dept. of Mechanical Engineering, University of Minnesota; [2] Dept. of Chemical Engineering and Materials Science, University of Minnesota

Motivation

- 60% of single-crystal (c-Si) based photo-voltaic costs come from expensive crystal wafer mfg. processes [1]
- Thin film amorphous silicon (a-Si) based cells, grown from silane dissociation in plasma (PECVD), reduce mfg. costs but have poor transport properties which degrade further with light exposure [2]
- Micro-crystalline silicon (µc-Si) based cells show improved transport and light stability over a-Si while maintaining the same cost advantage
- However, both transport properties and ease of processing must be improved further to be competitive with c-Si technologies

Background

- **Control of grain formation** = better control of transport properties; larger grains are more favorable for electronic transport
- **Reduced crystallization time** = improved processing costs
- µc-Si films are most easily obtained from solid-phase crystallization (SPC) of PECVD a-Si films at temperatures above 550C via the process of native nucleation
- Formation of native sites is dependant on many factors; can be difficult to control location/population-density of grains [3,4]

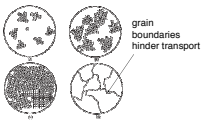

representation of native nucleation

Potential Solution

- Control location/density of crystal grain formation by pre-embedding crystallite "seeds" into the a-Si film

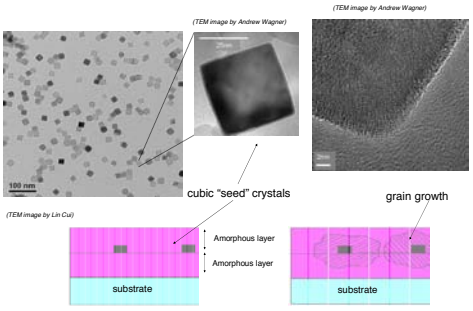

Acknowledgements

This work was partially supported by NSF grants DMR-0705675, NSF under MRSEC grant DMR-0819885, and by the Xcel Energy Renewable Development Fund under grant RD-3-25.
Parts of this work were carried out in the College of Science and Engineering Characterization Facility, University of Minnesota, which receives partial support from NSF through the MRSEC program

Process

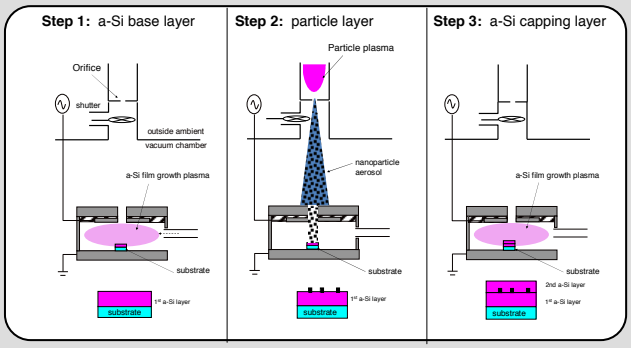

Results

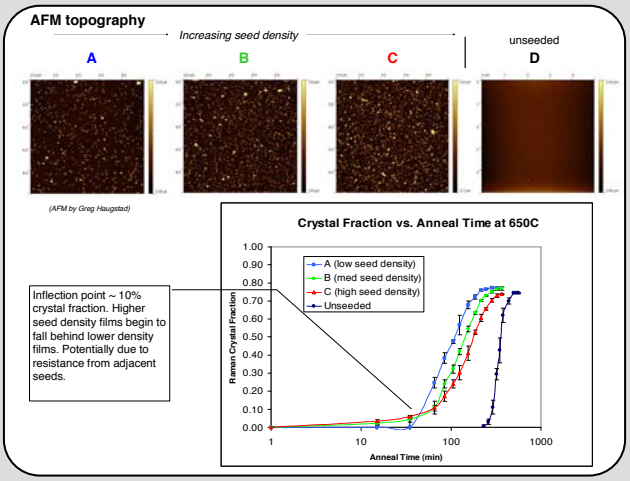

Inflection point ~ 10% crystal fraction. Higher seed density films begin to fall behind lower density films. Potentially due to resistance from adjacent seeds.

Future studies

- High seed density mono-layer = forced vertical column growth/through thickness grains?
- Mobility measurements of various structures
- Grain size/shape evaluation via EBSD
- Effect of different seed shapes on crystallization kinetics
- EELs/TEM in-situ analysis of crystallization mechanism

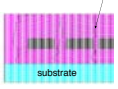

References

1. R.H. Buitrago, G.A. Risso, M. Cutrera, M. Battioni, L. De Bernardez, J.A. Schmidt, R.D. Arce, R.R. Koropecki, *Polycrystalline silicon thin film solar cells prepared by PECVD-SPC.* Int. J. of Hydrogen Energy, **33** (2008) 3522-3525
2. A. Koloziedj, *Staebler Wronski effect in Amorphous Silicon and its Alloys.* Opto-electronics Review **12**(1), 21-32 (2004)
3. R. B. Iverson and R. Reif, *Re-crystallization of amorphized polycrystalline silicon films on SiO2: Temperature dependence of the crystallization parameters.* J. Appl. Phys **62**, 5 (1987) 1675-1681.
4. C. Spinella and S Lombardo, *Crystal grain nucleation in amorphous silicon,* J. Appl. Phys. **84**, 10 (1998) 5383-5415.

High Temperature and Plasma Lab
Mechanical Engineering

UNIVERSITY OF MINNESOTA
Driven to Discover℠